

Structural Design and Compensation Control of Supernumerary Robotic Limbs for Overhead Work

LIU Keming¹, CHEN Bai^{1*}, XU Jiajun¹, JIANG Surong², LIU Debin¹,
CHANG Tianzuo¹, BAI Dongming^{3,4}

1. College of Mechanical and Electrical Engineering, Nanjing University of Aeronautics and Astronautics, Nanjing 210016, P. R. China;

2. College of Science, Nanjing University of Aeronautics and Astronautics, Nanjing 211106, P. R. China;

3. Mechanical & Electrical Engineering College, Jinhua Polytechnic, Jinhua 321016, P. R. China;

4. Key Laboratory of Crop Harvesting Equipment Technology of Zhejiang Province, Jinhua 321016, P. R. China

(Received 8 February 2023; revised 28 June 2023; accepted 10 September 2023)

Abstract: In order to reduce operator fatigue and accelerate aircraft cabin assembly, supernumerary robotic limbs (SRLs) are developed for overhead work in cabin assembly task. The SRLs assist workers in supporting the ceiling to achieve single-person operation via dual three-degree-of-freedom robotic limbs, which are mounted on the human shoulder. The proposed robot can replace the original two-person operation mode, which reduces labor costs and avoids the burden of supporting tasks on workers. A flexible saddle-liked wearable backpack and a flexible end-effector are designed to improve the wearing comfort and environmental adaptability. At the same time, to ensure the safety of human-robot collaboration, the SRLs are designed to address the issues by sensor detection, tendon-driven decoupling mode selection and motion parameter limitation. Moreover, a position compensation control algorithm is designed based on the ergonomic kinematics model to avoid the interference caused by human perturbation. A force compensation control algorithm is designed based on the admittance control principle to improve the operational stability. Experimental results show that the proposed position algorithm reduces the end position error by more than 74%, compared with the original error. The proposed force algorithm can control the single robotic limb of the SRLs to output target force of 5 N for meeting the requirement.

Key words: supernumerary robotic limbs; structural design; tendon-driven; position compensation; admittance control

CLC number: TP242.3

Document code: A

Article ID: 1005-1120(2023)06-0727-11

0 Introduction

The overhead work in aircraft cabin requires two-person cooperation, which is very easy to induce occupational musculoskeletal diseases and reduce the operation efficiency of workers^[1]. If the equipment can replace workers to complete the lifting task to achieve auxiliary overhead operation functions, it will reduce the work load and improve the operation efficiency in aircraft assembly task. Existing collaborative robots are often difficult to move

flexibly and autonomously in complex environments, while exoskeletons can only assist workers^[2-3]. For such cases, researchers have proposed a new robotic paradigm called supernumerary robotic limbs (SRLs)^[4-5]. SRLs can be used to expand or augment human's mobility, perception, operation and other abilities by robotic limbs that mounted on the human body^[2]. Therefore, SRLs are able to complete the lifting tasks and help workers to achieve one-man overhead work. However, it

*Corresponding author, E-mail address: chenbye@126.com.

How to cite this article: LIU Keming, CHEN Bai, XU Jiajun, et al. Structural design and compensation control of supernumerary robotic limbs for overhead work[J]. Transactions of Nanjing University of Aeronautics and Astronautics, 2023, 40(6): 727-737.

<http://dx.doi.org/10.16356/j.1005-1120.2023.06.009>

brings the challenges that design and control of SRLs^[3], because SRLs are very close to human body. For example, SRLs require high safety than conventional manipulator. The motion disturbance from human body is also a challenge that precise operation of SRLs^[6].

In the structural design of SRLs, researchers have mainly explored two directions: rigid and flexible structures. Bright et al.^[7] developed a five-degree-of-freedom rigid SRL for overhead work. It consists of two robotic limbs, a shoulder seat, electronic control, and sensing units, and each joint of the robot is driven by a servo motor. The SRL has problems with heavy weight and overly concentrated loads. Seo et al.^[8] also developed a three-degree-of-freedom serially connected SRLs for overhead operations. Its composition is similar to the former, but the structure is more compact and has a smaller load. To address the problem of poor load-bearing capacity of existing serially connected SRLs, Zhang et al.^[9] developed a reconfigurable SRL with serial and parallel structures, which can better adapt to different task requirements. Al-Sada et al.^[10] developed a flexible SRL for daily life scenarios. The SRL is different from the typical flexible SRLs' structure. Borrowing from the principle of snake deformation, it connects 25 rigid rotational joints in series to have enough flexibility to produce deformation and movement. Nguyen et al.^[11] designed flexible SRLs. The SRLs' manipulator borrows from the principle of elephant trunk deformation. It uses a connection method of first parallel and then serial with airbags to make the manipulator undergo complex deformation.

Currently, the main structure of SRLs for overhead work is rigid^[12]. The rigid SRLs have the advantages of high structural strength, large load capacity, and high precision. But they are heavy and have a large moment of inertia, as well as poor safety and comfort when worn^[13-14]. On the other hand, existing flexible SRLs are mainly used in daily scenarios, with lighter weight and higher safety, but there are disadvantages such as difficult control, slow response, and low control precision^[15-16]. Based on previous research, this paper designs a

three-degree-of-freedom rigid SRL worn on the human shoulder. The structure arranges all joint motors on the backplate and drives the joints through tendon-drive, which has the advantages of rigid-flexible coupling and greatly reduces the movement inertia during operation. In addition, the contact part between the SRLs and the human shoulder is designed with a flexible saddle to improve the comfort of wearing. The interaction safety of the SRLs is improved by limiting the maximum joint angle, designing a sensing detection outer wall, and choosing a rope drive decoupling method.

For the problem of accurate control of the end position and force of the SRLs under human perturbation, there are still relatively few studies^[17]. Bright et al.^[7] designed a perturbation compensation strategy based on end force sensors and impedance control for the SRLs in cabin cable deployment operation, and the experiments showed that the robot could maintain stable contact with the target point under perturbation by adjusting and controlling the end support force and friction force. Seo et al.^[8] designed a perturbation compensation method similar to the above for the SRLs of the overhead ceiling installation operation, based on the guide control method, and adjusted the robot end support force to reduce the perturbation error from 170 mm to 20 mm. Vatsal et al.^[18] explored closed-loop control of the end position using visual guidance technology, but this approach requires certain environmental conditions to be realized. This paper focuses on its position perturbation compensation method, and proposes a human-robot co-integration model. A position compensation method is designed for human perturbation, which is based on the above model and combined with robot inverse kinematics. In terms of force compensation control, this paper realizes closed-loop control of end force based on conductance control. Finally, an experimental platform is built to verify the effectiveness of the position/force compensation control algorithm.

This study's main contributions are presented as follows: (1) Tendon-driven SRLs are developed, and they are lighter and more safety than conventional SRLs and can reduce the human work-

load; (2) a position and force compensation algorithm are developed to reduce the disturbance from the human body and environment.

1 Design of SRLs

1.1 Structural design of SRLs

The flow of SRLs to assist the worker in overhead work is shown in Fig.1. First, the worker carries the ceiling to a fixed position and provides manual support. Next, the SRLs are moved to a preset support position by human voice commands and one-handed gesture commands^[2]. Then, the worker releases the hands and the SRLs are supported individually. Finally, the worker picks up the tools to carry out the installation work on the ceiling. Clearly, the floating base of the SRLs due to human perturbation affects its end-stable support and it is important to develop a position/force compensation algorithm. In this paper, the mass of the ceiling for the task is set to 1 kg and the output force of the single-limb steady support is not less than 5 N. In addition, the process does not require any movement of the human lower limbs in order to reduce the complexity of the human disturbance compensation algorithm.

In view of the requirements of assisting overhead operation, this paper designs a lightweight, portable and safe dual robotic limbs of the SRLs. As shown in Fig.2, the SRLs are mainly composed of a flexible saddle, two robotic limbs in a symmetrical configuration of left and right, and wearable control system. For the sake of lightweight, the robotic limb is made of carbon fiber board, and the overall system mass is 6.5 kg, which is an acceptable

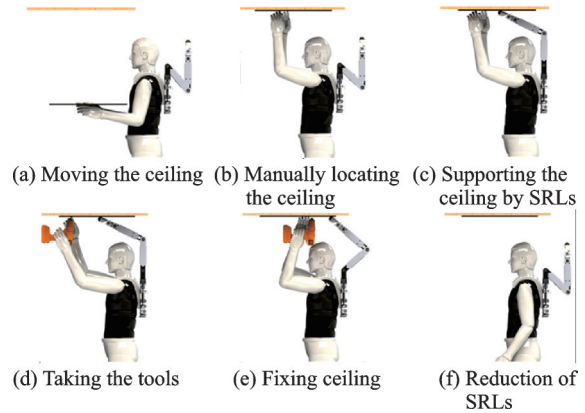


Fig.1 Assist in creating the workflow diagram for the project

weight for the human. Each robotic limb of the SRLs mainly consists of a base, a large arm, a small arm and a flexible end-effector, with a total length of 730 mm. The body of the robotic limb is made of carbon fibre with a high strength ratio and weighs approximately 1.25 kg. The rated load on one robotic limb is 0.5 kg and the maximum load on one robotic limb does not exceed 1.5 kg. The elastic telescopic column arranged in an array is designed for the contact between the SRLs and the human body. On the one hand, the design can automatically adapt to the shape and structure of the human shoulder. On the other hand, the design can effectively reduce stress concentration and improve wearing comfort.

The base and the robotic limb are connected by three rotary joints, of which joint 1 is driven by direct motor drive, while the motors of joints 2 and 3 are placed on the back plate and driven by tendon, which greatly reduces the inertia of motion during the work of the SRLs and reduces the reaction force of the SRLs on the human body. The way in which

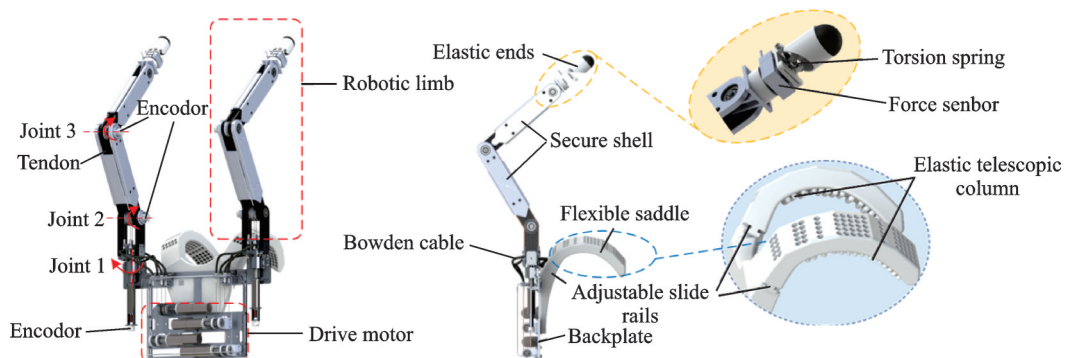


Fig.2 Structure design of SRL

the rope is driven also affects the accuracy of the robot's movement. The measured positioning accuracy of the SRLs is ± 8 mm and the repeat positioning accuracy is 25—30 mm. However, this does not affect the movement of the SRLs to the target position, and the end position of the SRLs can be fine-tuned by gesture control^[2]. An elastic end effector is designed, which contains a rotating joint with a built-in torsion spring, the structure can produce elastic deformation when the end force changes, so that the SRLs show good compliance during work. A force sensor is also mounted on the bottom of the actuator to detect the end force.

1.2 Safety design of SRLs

In view of the safety problem in human-robot collaboration, SRLs have been designed accordingly in sensing detection, tendon-driven decoupling mode selection and motion parameter limitation.

Based on the principle of pressure sensing, a safety shell mounted on the robotic limb is designed. The principle is shown in Fig.3. The safety shell and the SRLs are connected by wave springs. There are protruding contacts on the safety shell. A thin-film pressure sensors is arranged directly below the contacts. When there is no human-robot collision, the contact is in a suspended state, and the pressure sensor does not respond. When a human-robot collision occurs, the wave spring is compressed, and the pressure sensor responds quickly. Then, the robotic limb immediately stops moving and makes obstacle avoidance response actions under program control.

To avoid inter-articular motion coupling, the Bowden cable transmission is adopted at joint 1 (Fig.2) for the transition when winding. One of the

characteristics of the Bowden cable transmission method is the large friction, and this paper cleverly uses this feature. When the SRLs are unexpectedly powered off, the robotic limb and the ceiling will be subjected to the reverse cushioning force during the hanging process, which greatly reduces the damage to the human body by collision.

In addition, this paper limits the maximum range of allowable rotation of the three joints of the SRLs^[19], namely: $-90^\circ - 90^\circ$, $-135^\circ - 135^\circ$, $-135^\circ - 135^\circ$. The measure fundamentally avoids the infringement of the robotic limb on the head space.

2 Position /Force Compensation Control of SRLs

2.1 Position compensation control algorithm

2.1.1 Compensatory control strategy based on robot inverse kinematics

In this paper, the human body and the SRLs are integrated into a whole, and a human-robot integration model as shown in the left of Fig.4 is established. The model can effectively predict and compensate for the terminal motion error of the SRLs caused by human disturbance. Based on the process of using SRLs as assistance in work, this paper assumes that the lower limbs of the human body are restricted to a fixed position. This condition serves as a prerequisite for establishing a human-robot symbiosis model. The inverted triangle area in the figure represents the fixed connection between the human and machine. The leg linkages are fixed to the ground, and the waist joint is simplified as a ball

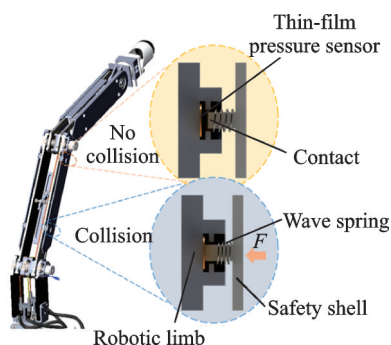


Fig.3 Safety principle of the SRLs' shell

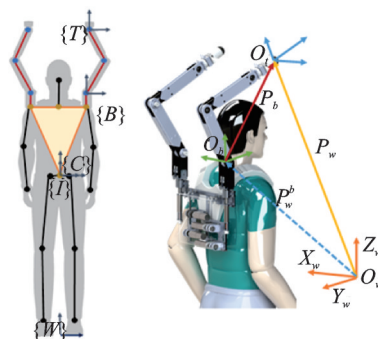


Fig.4 Human-robot integration model

joint rotating around the center point of the waist. $\{W\}$ is the world coordinate system fixed to the ground, with the origin coinciding with the intersection of the human body's central axis and the ground. $\{C\}$ is the waist center coordinate system fixed to the center point of the sacrum, and waist movement can be simplified as rotational movement around the X and Y axes of this system. $\{I\}$ is a simplified carrier coordinate system connected to the rigid bone structure of the back, and the attitude angle measured by the inertial sensor is the rotation angle of this system around the three coordinates axes of $\{C\}$. $\{B\}$ is the base coordinate system of the SRLs, and $\{T\}$ is the coordinate system of the center of the end effector of the SRLs.

The target position of the robot is given in the form of coordinates P_w in the world coordinate system. But the final control of the robot is relative to its position of the base coordinate system P_b , and the relationship between them is shown in Fig.4. Therefore, this paper designs an inverse kinematics compensation strategy based on the human-robot integration model. The real-time calculation result of the robotic target point under the robotic base system can be expressed as

$$\begin{aligned} \begin{bmatrix} P_t^b \\ 1 \end{bmatrix} &= H_w^b \begin{bmatrix} P_t^w \\ 1 \end{bmatrix} = [H_b^w]^{-1} \begin{bmatrix} P_t^w \\ 1 \end{bmatrix} = \\ &H_b^{i-1} H_i^{c-1} H_c^{w-1} \begin{bmatrix} P_t^w \\ 1 \end{bmatrix} \end{aligned} \quad (1)$$

where H_b^w represents the coordinate transformation relationship of the robot base coordinate system $\{B\}$ relative to the world coordinate system $\{W\}$, H_w^b the coordinate transformation relationship of the world coordinate system $\{W\}$ relative to the robot base coordinate system $\{B\}$, H_b^{i-1} the coordinate transformation relationship of the robot base coordinate system $\{B\}$ relative to the carrier coordinate system $\{I\}$ at the last moment, H_i^{c-1} the coordinate transformation relationship of the carrier coordinate system $\{I\}$ relative to the waist center system $\{C\}$ at the last moment, and H_c^{w-1} the coordinate transformation relationship of the central system $\{C\}$ of the waist relative to the world coordinate system $\{W\}$ of the last moment; P_t^b and P_t^w represent the coordi-

nates of the end points in the robot base coordinate system $\{B\}$ and the world coordinate system $\{W\}$, respectively.

The real-time solution of the end point in Eq.(1) under the robot base system includes the human disturbance term H_i^{c-1} , and the solution result is the compensated robot end trajectory.

2.1.2 Solving for compensating posterior joint angles

After the terminal trajectory of the SRLs in the base coordinate system is obtained through the above transformation, the target trajectory of the robot in the joint space can be obtained by using the robot inverse kinematics solution. In this paper, the coordinate system of each connecting rod of the SRLs is constructed based on the D-H parameter method, as shown in Fig.5. In Fig.5, x_0, y_0, z_0 represent the specific form of the base coordinate system $\{B\}$; x_i, y_i, z_i ($i=1, 2, 3$) the specific form of the link coordinate system; x_t, y_t, z_t the specific form of the base coordinate system $\{T\}$; a_2, a_3 the lengths of the SRLs' upper and lower arm, respectively; and $\theta_1, \theta_2, \theta_3$ the output angles of each joint. The D-H parameters of each connecting rod are shown in Table 1.

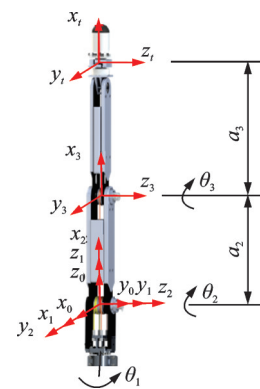


Fig.5 Illustration of the coordinate system of the SRLs' linkage

Table 1 D-H parameters of each linkage of SRLs

Connecting rod i	$\theta_i / (^\circ)$	$\alpha_{i-1} / (^\circ)$	a_{i-1} / mm	d_i / mm
1	0	0	0	0
2	-90	-90	0	0
3	0	0	250	0
T	0	0	330	0

In the process of robot forward kinematics solution, it is known that the robot forward kinematics solution matrix has the following form

$$H_t^b = \begin{bmatrix} \mathbf{R}_t^b(\theta) & \mathbf{P}_t^b \\ 0 & 1 \end{bmatrix} = \begin{bmatrix} c_1 c_{23} & -c_1 s_{23} & -s_1 & P_x \\ s_1 c_{23} & -s_1 s_{23} & c_1 & P_y \\ -s_{23} & -c_{23} & 0 & P_z \\ 0 & 0 & 0 & 1 \end{bmatrix} \quad (2)$$

where $\mathbf{R}_t^b(\theta)$ denotes the rotation coordinate matrix of the point of the end of SRLs with respect to the base coordinate system $\{B\}$ of SRLs; c_1 , s_1 , s_{23} , and c_{23} are abbreviations for $\cos \theta_1$, $\sin \theta_1$, $\sin(\theta_2 + \theta_3)$, and $\cos(\theta_2 + \theta_3)$, respectively; $\mathbf{P}_t^b = [P_x P_y P_z]^T$, $P_x = c_1(a_2 c_2 + a_3 c_{23})$, $P_y = s_1(a_2 c_2 + a_3 c_{23})$, $P_z = -a_3 s_{23} - a_2 s_2$, here a_2 and a_3 are lengths of the large arm and the small arm of the SRLs, respectively.

The transformation matrix of each connecting rod is multiplied to obtain the closed-loop matrix of the robotic limb of the SRLs, shown as

$${}^0T = {}^0T(\theta_1) {}^1T(\theta_2) {}^2T(\theta_3) {}^3T(0) \quad (3)$$

In the process of solving the robot joint angle, the unknown link inverse transformation is used to multiply both sides of Eq.(3) from the left, which can separate the robot joint variables for further solution. Finally, a set of joint angle data is used to compensate the robot in real time.

The principle of the position compensation algorithm can be represented in the form shown in Fig.6. It consists of a series control loop that compensates for the positional error in the human-robot co-adaptive model coordinate system by converting the positional changes of the SRLs' base coordinate system caused by human disturbances. This greatly improves the positional control accuracy of the SRLs during overhead operations. Here, \mathbf{X}_s represents the position of the SRLs' target point in the world coordinate system; \mathbf{X}_c and \mathbf{X}_d represent the actual position of the SRLs' end point in the world coordinate system and the base coordinate system, respectively; $\Delta \mathbf{X}_c$ and $\Delta \mathbf{X}_d$ represent the expression of the difference between the target position of the SRLs and the actual position of the end point in the world coordinate system and the base coordinate system, respectively; $\Delta \mathbf{q}_i$ represents the compensation required for joint angles, and \mathbf{q}_i the actual joint

angles feedback from the encoder; ${}^0T(\theta_i)$ and ${}^0T^{-1}(\theta_i)$ represent the forward and inverse kinematics of the SRLs, respectively. The red box represents the coordinate transformation method based on the human-machine co-adaptive model, and $H_c^w H_i^c H_b^i$ and $H_b^{i-1} H_i^{c-1} H_c^{w-1}$ represent the homogeneous transformation and the homogeneous inverse transformation for converting the end point from the base coordinate system to the world coordinate system.

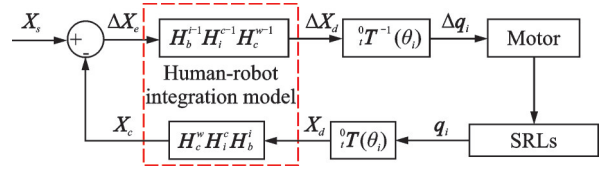


Fig.6 Position compensation control diagram

2.2 Force compensation control algorithm

When the end of the SRLs is in contact with the environment, the control requirements of the SRLs are changed to the soft control of the terminal force. Admittance control can not only ensure that the robot works in a constrained environment, but also maintain appropriate interaction force. At the same time, it has strong robustness to uncertainties and external interference. Therefore, this paper realizes closed-loop control of the SRLs terminal force based on admittance control. The admittance controller monitors the error between the end force and the target force, and adjusts the position of the end of the SRLs based on the obtained force error, so that the end of the SRLs maintains the ideal interaction force with the environment. The architecture of the SRLs' admittance control is shown in Fig.7, where F_{ext} represents the external force, \mathbf{x}_0 the initial target position, and \mathbf{x}_d the target position output by the comprehensive admittance characteristics.

The innermost loop of the servo motor controller used in the SRLs of this paper adopts a speed control ring. In order to achieve a better control effect, the admittance control law finally used in this paper can be expressed as

$$\Delta V = \mathbf{K} \times \Delta F \quad (4)$$

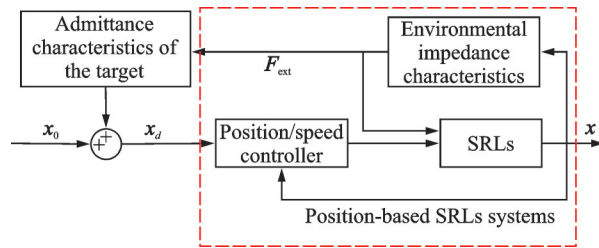


Fig.7 Force compensation control diagram

where $\Delta V = [\Delta v_x, \Delta v_y, \Delta v_z]^T$ is the component of the terminal velocity of the robot, $\Delta F = [\Delta f_x, \Delta f_y, \Delta f_z]^T$ the component of the force at the end of the robot, and $K = \text{diag}[k_1, k_2, k_3]$ the feedback coefficient of ΔF relative to ΔV .

3 Compensation Control Algorithm Verification Experiment

The SRLs' control experimental platform is built to verify the effect of position/force compensation control algorithm, as shown in Fig.8. The terminal position/force control experiment under human disturbance is completed based on this platform. During the experiment, the operator interacts with the SRLs through voice command. The experimental platform is composed of host and client, the SRLs' prototype and laser tracker system.

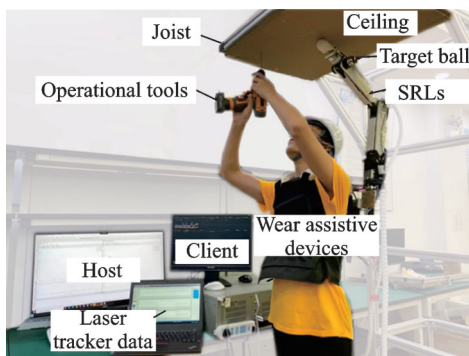


Fig.8 Experimental platform of SRLs

3.1 Position compensation control algorithm verification experiment

In order to evaluate the effect of the SRLs' position compensation control algorithm, this paper conducts a control verification experiment, which is mainly divided into two parts: Active compensation experiment and control experiment. In the active

compensation experimental part, the human waist is controlled to move sequentially in two directions: Backward pitch, and left and right deflection. The position compensation control algorithm is used to control the terminal movement of the robot, and the target point of control is a fixed point in the world coordinate system. In the control experiment part, only the control algorithm used by the robot is modified, and other factors are the same as the active compensation experiment. During the experiment, the laser tracker system is used to track the end position of the robot during the experiment, and the change trajectory of the end position coordinates over time and the distribution in space are obtained.

The change of the component of the SRLs' end trajectory in the three-coordinate axis direction measured under the perturbation law is shown in Fig.9. The distribution range of the position error of the experimental group e_e , the position error of the control group e_c in the three-coordinate direction and the maximum amplitude ratio A_{\max} are shown in Table 2. The expression for the maximum amplitude ratio can be expressed as

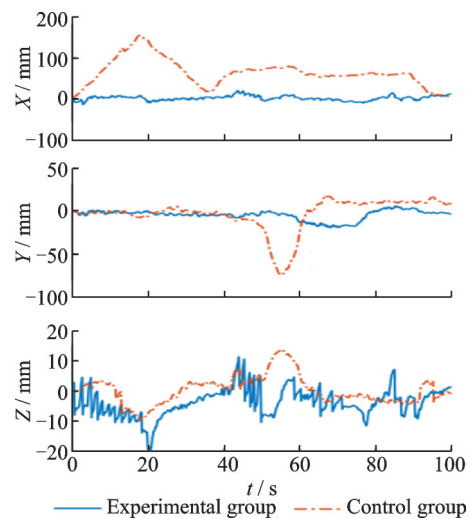


Fig.9 End trajectories of the experimental group and the control group

Table 2 Trajectory error data for experimental group and control group

Projection direction	e_e/mm	e_c/mm	$A_{\max}/\%$
X	0—155.69	-12.66—20.07	13
Y	-73.37—18.96	-19.04—5.92	26
Z	-10.02—13.64	-19.82—11.34	145

$$A_{\max} = \frac{|e_c|_{\max}}{|e_t|_{\max}} \times 100\% \quad (5)$$

The experimental results show that the SRLs in the X and Y directions produce a large perturbation error. The X and Y directions are the error-sensitive direction. In the control group, the main perturbation error in the X direction occurs during the back and forth pitching of the human body, and its deviation range is reduced to 13% of the original error after position compensation. The main perturbation error in the Y direction occurs during the left and right deflection of the human body, and its deviation range is reduced to 26% of the original error. This shows that the position compensation algorithm has a significant compensation effect in the error-sensitive direction, reducing the original error by more than 74%.

No significant perturbation occurs in Z -direction. After position compensation, its trajectory shows pulse-type fluctuation, and the error range is further expanded instead. This phenomenon is related to the tendon-drive, as shown by the trajectory change of the Z -direction end in Fig.9. The SRLs of the control group completed a joint change at 18 s, but in the experimental group, the joint change of the SRLs occurred at about 20 s. It is due to the delay and return error of the joint control^[8] caused by the deformation of the robot's tendon during the position compensation, and the tendon produced further deformation in 18–20 s. This leads to a negative effect of Z -directional position compensation.

3.2 Force compensation control algorithm verification experiment

A closed-loop force control experiment of the SRLs is designed, in order to evaluate the force control effect of the SRLs when it is in contact with the ceiling. The experiment is still carried out in the platform shown in Fig.8. The difference is that the data obtained from the force control experiment is collected by a force sensor at the end of the robot. The terminal force change curves are shown in Fig.10.

The data in the range of 0–140 s in Fig.10 re-

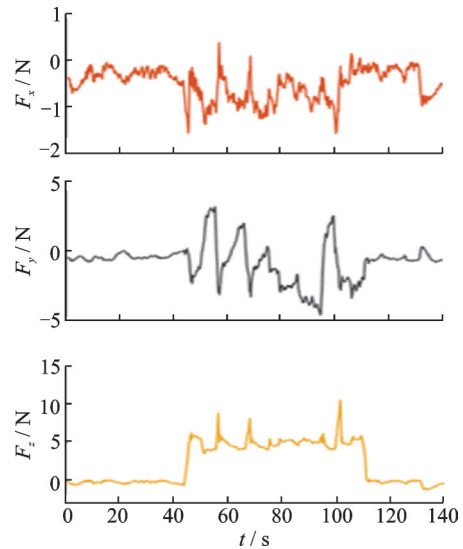


Fig.10 Curves of terminal force change in force control experiment

cord the change of the interaction force between the SRLs and the ceiling, when the SRLs contact the ceiling, stably support, and then detach from the support. From the actual contact force F_z with time, it can be seen that the contact process between the SRLs and the ceiling is relatively stable, and there is no obvious impact. The overall force in the support state is maintained at about 5 N of the target force, which ensures reliable support force output. In the stable support process of 48–108 s, there are three obvious impulse mutations in F_z . Through the disturbance analysis at the moment of sudden force mutation, it can be seen that the direction of human disturbance at this moment has abruptly changed, and the position error caused by the joint adjustment lag and return error of the tendon-drive will eventually be manifested as a force control error through the conduction at the end. It will eventually lead to the rise of the support force F_z and the friction force F_x, F_y . However, under the adjustment of the admittance controller, the end force will eventually return to the vicinity of the target force. Therefore, the change in terminal force will eventually manifest itself as a short rise and eventually return to stability as shown. But this situation does not affect the support effect of the SRLs on the ceiling.

4 Conclusions

A lightweight and safety SRLs' system is designed based on the tendon-driven module to meet the needs of overhead auxiliary operations in aircraft cabin. In terms of structural design, an elastic end effector is designed in order to increase the flexibility of the end support structure of the SRLs. The flexible saddle is designed to adapt to the shoulder shape of different users with improving wearing comfort and adaptability. The safety of the human-robot system is improved from three aspects: A flexible shell is designed for collision detection; the Bowden cable is designed as a decoupling method for the tendon-drive, and it can provide buffer protection when the system is accidentally powered off due to its high friction; accordingly, the maximum range of rotation allowed for the three joints of the SRLs is limited.

Aiming at the unique dynamic base problem of the SRLs, this paper integrates the human body and the SRLs into a whole, constructs a human-robot integration model, and transforms the dynamic base problem into a fixed base problem. Then, a position/force compensation control algorithm is proposed for the SRLs on this basis, which is verified by experiments. Experimental results show that the position compensation algorithm used in this paper has obvious compensation effect in the error-sensitive direction, and the position error is controlled within 30 mm, which is more than 74% less than the original error. The position compensation algorithm achieves the effect of stabilizing the terminal position of the SRLs and improves the control accuracy of the SRLs. The force compensation control algorithm stabilizes the interaction force as a whole near the target force, which can ensure the rated support force output of 5 N for one robotic limb. The experimental results also show that the joint motion delay and angle abrupt change phenomenon has an impact on the further improvement of the control accuracy. The phenomenon is caused by the tendon-driven technology during the joint commuta-

tion. In the subsequent study, the deformation of the tendon will be added into the position error compensation algorithm to improve the flexibility and tracking accuracy of the SRLs by further optimization to achieve better control effect.

A control experiment platform based on Simulink Real-Time in MATLAB environment is used to verify the effectiveness of the control algorithm. This approach requires the multiple computers for accurate control and long cable connection between the SRLs and the controller, which limits the passing performance of the SRLs. In subsequent improvements, a highly integrated embedded controller and a signal transmission method with wireless transmission can be used to further enhance the portability of the SRLs.

References

- [1] SUN J H, CHANFIOU A M, WANG Y, et al. A review on effects of personalized ventilation systems on air quality and thermal comfort in aircraft cabin mini environments[J]. *Transactions of Nanjing University of Aeronautics and Astronautics*, 2022, 39(2): 121-142.
- [2] LIU D B, WANG D, CHEN B, et al. A survey of supernumerary robotic limbs[J]. *Journal of Zhejiang University (Engineering Science Edition)*, 2021, 55(2): 251-258.
- [3] LIAO Z Y, CHEN B, ZHENG Q, et al. Collaborative workspace design of supernumerary robotic limbs base on multi-objective optimization[J]. *Journal of the Brazilian Society of Mechanical Sciences and Engineering*, 2023, 45: 354.
- [4] LLORENS-BONILLA B, PARIETTI F, ASADA H H. Demonstration-based control of supernumerary robotic limbs[C]//*Proceedings of the 25th IEEE/RSJ International Conference on Intelligent Robots and Systems (IROS)*. Portugal: IEEE, 2012: 3936-3942.
- [5] TONG Y C, LIU J G. Review of research and development of supernumerary robotic limbs[J]. *IEEE/CAA Journal of Automatica Sinica*, 2021, 8(5): 929-952.
- [6] YANG B, HUANG J, CHEN X X, et al. Supernumerary robotic limbs: A review and future outlook[J]. *IEEE Transactions on Medical Robotics and Bionics*, 2021, 3(3): 623-639.
- [7] BRIGHT Z, HARRY A H. Supernumerary robotic limbs for human augmentation in overhead assembly

- tasks[C]//Proceeding of Robotics: Science and Systems VIII. [S.I.]: RSS, 2017.
- [8] SEO W, SHIN C Y, CHOI J, et al. Applications of supernumerary robotic limbs to construction works: Case studies[C]//Proceedings of ISARC 2016 33rd International Symposium on Automation and Robotics in Construction. Auburn: IAARC, 2016: 1041-1047.
- [9] ZHANG Q H, LI C L, JING H W, et al. RTSRAs: A series-parallel-reconfigurable tendon-driven supernumerary robotic arms[J]. IEEE Robotics and Automation Letters, 2022, 7(3): 7407-7414.
- [10] AL-SADA M, HÖGLUND T, KHAMIS M, et al. Orochi: Investigating requirements and expectations for multipurpose daily used supernumerary robotic limbs[C]//Proceedings of the 10th Augmented Human International Conference 2019. Reims France: ACM, 2019: 1-9.
- [11] NGUYEN P H, SPARKS C, NUTHI S G, et al. Soft poly-limbs: Toward a new paradigm of mobile manipulation for daily living tasks[J]. Soft Robotics, 2019, 6(1): 38-53.
- [12] DANIEL P H, FU C L, ASADA H H. Musculoskeletal load analysis for the design and control of a wearable robot bracing the human body while crawling on a floor[J]. IEEE Access, 2022, 10: 6814-6829.
- [13] LIAO Z Y, CHEN B, CHANG T Z, et al. A human augmentation device design review: Supernumerary robotic limbs[J]. Industrial Robot: The International Journal of Robotics Research and Application, 2023, 50(2): 256-274.
- [14] LIU S C, ZHU Y H, ZHANG Z C, et al. Otariidae-inspired soft-robotic supernumerary flippers by fabric kirigami and origami[J]. IEEE/ASME Transactions on Mechatronics, 2021, 26(5): 2747-2757.
- [15] LIANG X Q, CHEONG H, CHUI C K, et al. A fabric-based wearable soft robotic limb[J]. Journal of Mechanisms and Robotics—Transactions of the ASME, 2019, 11(3): 031003.
- [16] SHAFTI A, HAAR S, MIO R, et al. Playing the piano with a robotic third thumb: Assessing constraints of human augmentation[J]. Scientific Reports, 2021, 11(1): 21375.
- [17] CUI S P, SUN Y J, LIU Y W, et al. Unified vibration suppression and compliance control for flexible joint robot[J]. Transactions of Nanjing University of Aeronautics and Astronautics, 2021, 38(3): 361-372.
- [18] VATSAL V, HOFFMAN G. End-effector stabilization of a wearable robotic arm using time series modeling of human disturbances[C]//Proceedings of ASME 2019 Dynamic Systems and Control Conference. Park City: AMSE, 2019.
- [19] CHANG T Z, JIANG S R, CHEN B, et al. Design of supernumerary robotic limbs and virtual test of human-machine interaction safety[M]//Proceedings of Advances in Mechanical Design. Singapore: Springer Nature Singapore, 2022: 2027-2045.

Acknowledgements This work was supported by the Fundamental Research Funds for the Central Universities (Nos. NP2022304, U22A20204), and the National Natural Science Foundation of China (Nos.52105103, 52205018).

Authors Mr. LIU Keming received the B.S. degree in mechanical engineering from Nanjing University of Aeronautics and Astronautics, Nanjing, China, in 2021. He is now a M.S. candidate in Nanjing University of Aeronautics and Astronautics, Nanjing, China. His research interests are wearable robot and variable stiffness joint.

Prof. CHEN Bai received the Ph.D. degree at Zhejiang University in 2005. Now he is a professor at College of Mechanical and Electrical Engineering, Nanjing University of Aeronautics and Astronautics. His current research interests include minimally invasive neurosurgery robot, virtual surgery system, force feedback control, and wearable robot.

Author contributions Prof. CHEN Bai contributed to the background of the study and designed the study. Mr. LIU Keming compiled the models and wrote the manuscript. Prof. XU Jiajun contributed to the discussion and revision of the study. Prof. JIANG Surong and Mr. LIU Debin deduced the mathematical model and assisted in the experiment. Dr. CHANG Tianzuo contributed to the discussion and background of the study. Dr. BAI Dongming contributed to the design and discussion of the study. All authors commented on the manuscript draft and approved the submission.

Competing interests The authors declare no competing interests.

过顶作业外肢体机器人结构设计与补偿控制研究

刘珂铭¹, 陈 柏¹, 徐嘉骏¹, 蒋素荣², 刘德斌¹, 常天佐¹, 白东明^{3,4}

(1. 南京航空航天大学机电学院, 南京 210016, 中国; 2. 南京航空航天大学理学院, 南京 211106, 中国;

3. 金华职业技术学院机电工程学院, 金华 321016, 中国;

4. 浙江省农作物收获装备技术重点实验室, 金华 321016, 中国)

摘要: 为了提高航空装配的效率, 开发了一种外肢体机器人用于飞机舱内的过顶作业。外肢体机器人(Supernumerary robotic limbs, SRLs)通过安装在人类肩膀上的三自由度机械臂, 协助工人支撑天花板, 实现单人作业, 这种方法取代了原来的双人作业模式, 降低了劳动成本, 减少了工人的负担。为提升穿戴舒适性与环境适应性, 分别设计了柔性鞍座与柔性末端执行器; 同时, 通过3种手段实现人机系统的安全性, 包括设计碰撞检测外壳、选择套索传动的绳驱动解耦方式和限制关节转角。针对辅助过顶支撑作业中动基座问题对外肢体位置/力控制造成的干扰, 构建了人机共融运动学模型, 基于此设计了位置补偿控制算法, 同时基于导纳控制原理设计了力补偿控制算法。实验测试结果表明, 所设计的位置补偿算法使末端位置误差较原始误差减小74%以上, 力控补偿算法可控制外肢体单臂以5 N的目标力恒定输出, 满足其作业需求。

关键词: 外肢体机器人; 结构设计; 绳驱动; 位置补偿; 导纳控制